iScience

CellPress
OPEN ACCESS

Review

Supramolecular enzyme-mimicking catalysts self-assembled from peptides

Qing Liu,[1,*] Akinori Kuzuya,[1] and Zhen-Gang Wang[2,*]

SUMMARY

Natural enzymes catalyze biochemical transformations in superior catalytic efficiency and remarkable substrate specificity. The excellent catalytic repertoire of enzymes is attributed to the sophisticated chemical structures of their active sites, as a result of billions-of-years natural evolution. However, large-scale practical applications of natural enzymes are restricted due to their poor stability, difficulty in modification, and high costs of production. One viable solution is to fabricate supramolecular catalysts with enzyme-mimetic active sites. In this review, we introduce the principles and strategies of designing peptide-based artificial enzymes which display catalytic activities similar to those of natural enzymes, such as aldolases, laccases, peroxidases, and hydrolases (mainly the esterases and phosphatases). We also discuss some multifunctional enzyme-mimicking systems which are capable of catalyzing orthogonal or cascade reactions. We highlight the relationship between structures of enzyme-like active sites and the catalytic properties, as well as the significance of these studies from an evolutionary point of view.

INTRODUCTION

Various naturally occurring enzymes, which feature remarkable catalytic efficiency and substrate specificity, can catalyze biochemical reactions under mild conditions and play a central role in the vast majority of *in vivo* metabolic processes.[1–4] Except for a few ribozymes[5–7] and deoxyribozymes,[8–10] most natural enzymes in living organisms are proteinaceous enzymes that are folded by one or more polypeptide chains. These polypeptides are composed of at most twenty types of common amino acids and two rare amino acids (selenocysteine[11,12] and pyrrolysine[13]). The sequences of those amino acids composing the polypeptides are defined as the primary structures of peptides. The peptides can form the secondary structures (e.g., α-helixes, β-sheets, or random coils) and the tertiary folding structures of the enzymes. In some enzymes, each polypeptide chain acts as a subunit and self-assembles into a high-order quaternary structure. About one-third of extant natural enzymes take metallic ions[14] as cofactors to provide thermodynamic fundamentals for the catalytic processes.

The secondary, tertiary, and quaternary structures of proteinaceous enzymes are maintained by noncovalent interactions, such as hydrogen-bonding, electrostatic, hydrophobic, π-π stacking, van der Waals interactions, or metal-ligand coordination. The disulfide bonds also contribute to the folding structures of some enzymes.[15] The excellent catalytic repertoire of extant natural enzymes is attributed to the unique chemical composition and three-dimensional pocket of their active sites, as a result of long-term evolutionary process.[16,17] Owing to the extraordinary catalytic efficiency and outstanding stereoselectivity, enzymes have been broadly applied in the fields of bioengineering,[18–21] biomedicine,[22–24] food production,[25,26] etc. However, the large-scale practical applications of enzymes are restricted. On one hand, most proteinaceous enzymes are susceptible to the environmental changes, especially the harsh conditions that may occur in the manufacturing process, such as high temperature, acidification/alkalization treatments, and organic solvents. On the other hand, up to now, the discovered natural enzymes are limited in the types of chemical reactions they catalyze to maintain the cell surviving, and it is difficult to modify the enzymes because of the complexity of their architectures. Moreover, extraction and purification of natural enzymes are generally high cost and time consuming.

The peptides, as fundamental building blocks of life, possess biocompatibility, programmability, as well as abundant noncovalent-bond donors/acceptors, for self-assembling into functional supramolecular

[1]Department of Chemistry and Materials Engineering, Kansai University, Yamate-cho 3-3-35, Suita, Osaka 564-8680, Japan

[2]State Key Laboratory of Organic-Inorganic Composites, Key Lab of Biomedical Materials of Natural Macromolecules (Beijing University of Chemical Technology, Ministry of Education), Beijing Laboratory of Biomedical Materials, College of Materials Science and Engineering, Beijing University of Chemical Technology, Beijing 100029, China

*Correspondence: liuqingucas@163.com (Q.L.), wangzg@mail.buct.edu.cn (Z.-G.W.)

https://doi.org/10.1016/j.isci.2022.105831

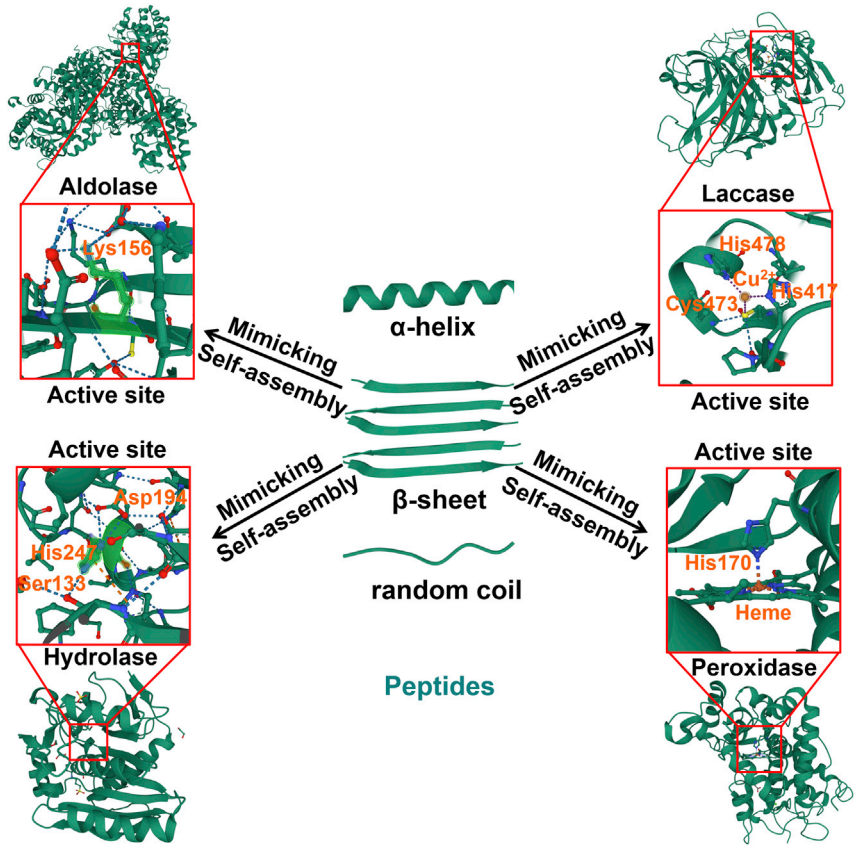

Figure 1. Constructing peptide-based supramolecular biomimetic artificial enzymes by emulating the active sites of natural enzymes

(PDB code: 1F2J (aldolase), 1V10 (laccase), 1H58 (peroxidase), 1H58 (hydrolase)).

materials. Inspired by the natural enzymes, a large number of peptide-based supramolecular catalysts have been constructed during the last decades.[27–32] In this review, we introduce the design principle of the peptide-based supramolecular catalysts, by focusing on some representative peptide-based biomimetic enzymes, including aldolases, laccases, peroxidases, and hydrolases (mainly the esterases and phosphatases). We also discuss some typical multifunctional peptide-based catalytic systems that were capable of catalyzing orthogonal or cascade reactions. Finally, we conclude with the possible future directions and challenges in this field.

DESIGN PRINCIPLE OF THE PEPTIDE-BASED SUPRAMOLECULAR CATALYSTS

Molecular self-assembly is omnipresent in nature. Natural evolution has led to many kinds of supramolecular self-assembled paradigms, for example, cell membranes, DNA double helices, and proteins. The integrated entities as a result of spontaneous organization of simple components can be endowed with emergent functions that any individual element does not own, which can be indicated by the catalytic superiority of natural enzymes generated via folding of polypeptides. Functional groups on the side chains of the non-catalytic polypeptides (sometimes with cofactors) are drawn close and oriented precisely to form the active sites of the enzymes.

The peptide-based supramolecular catalysts are constructed aiming to mimic the chemical structures of the enzymatic active sites (Figure 1). Through elaborately designing the sequences of peptides and adjusting the ratios between the constituents (sometimes including the cofactors), the arrangements of functional groups in active sites along with the catalytic performances of artificial enzymes can be tailored. The intrinsic dynamic features of noncovalent interactions allow the architectures of the supramolecular artificial enzymes to be controlled by external stimuli such as pH changes, heating, light, and additives. In this way, the artificial enzymes can be switched reversibly between the catalytically active and inactive states.

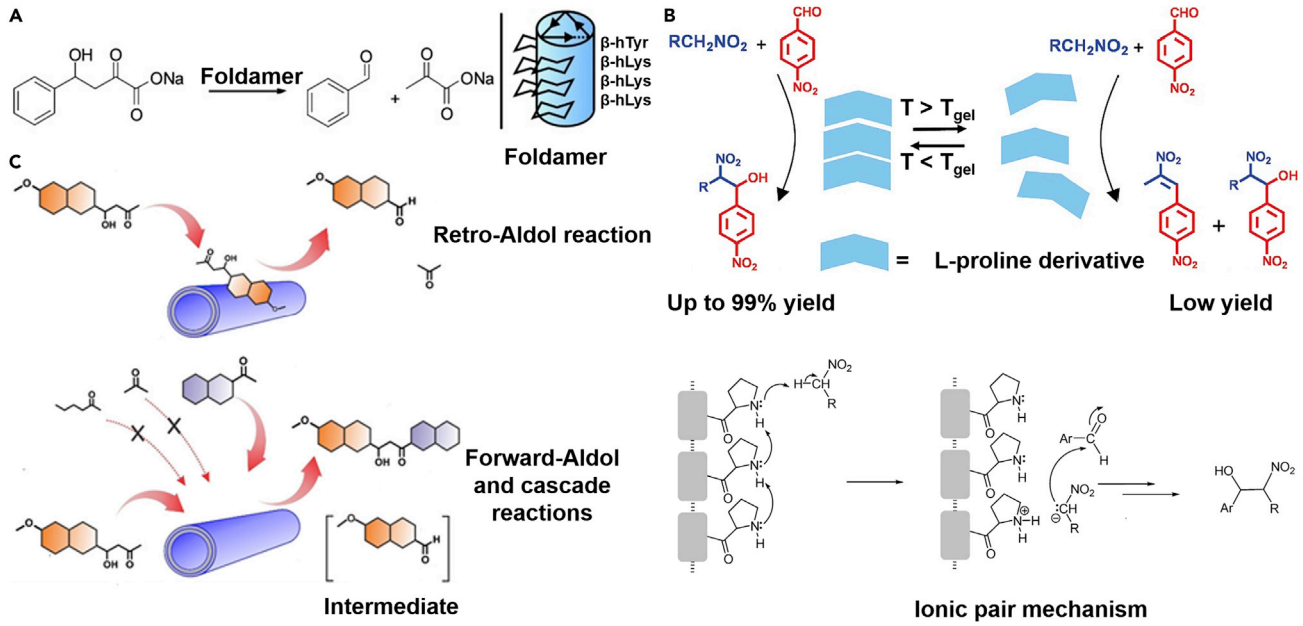

Figure 2. Representative peptide-based supramolecular aldolase mimics

(A) Retro-aldol cleavage of β-hydroxyketone to pyruvate and benzaldehyde catalyzed by a robust foldamer. Reproduced with permission from ref.,[40] copyright 2009, John Wiley & Sons, Inc..

(B) L-Pro-based temperature-responsive supramolecular gel catalyzed Henry aldol reaction and the reaction mechanism. Reproduced with permission from ref.,[41] copyright 2009, American Chemical Society.

(C) Self-assembled amyloid-like nanotube to catalyze forward aldol and retro-aldol reactions. Reproduced with permission from ref.,[42] copyright 2020, John Wiley & Sons, Inc..

It can be seen that the peptide self-assembly provides the possibility of constructing advanced enzyme-mimetic supramolecular catalysts. The underlying catalytic mechanisms of these systems are of great value in understanding correlation between the structures of active sites and the catalytic properties. This will benefit the development of artificial enzymes and shed light onto the evolution of natural enzymes.[33–35]

Aldolases

Aldolases can catalyze the formation/cleavage of carbon-carbon (C-C) bonds to yield miscellaneous organic molecules and play an important role in metabolic processes.[36,37] There are two kinds of naturally occurring aldolases, Class I and Class II aldolases, which have different architectures. Class I aldolases do not rely on any cofactor, while Class II aldolases require a metallic cofactor.[38] The structures and catalytic mechanism of Class I aldolases have been extensively studied due to their ubiquity and ease of purification.[39] Class I aldolases employ a multistep reaction mechanism, which involves the formation of a Schiff base between an active-site lysine (Lys) residue and a carbonyl group of substrate. Apart from the Lys in active site, C-terminal tyrosine (Tyr) residue can also act as hydrogen-bond donor to assist the catalytic reactions.

Inspired by the active sites of natural Class I aldolases and catalytic mechanism, a variety of peptide-based supramolecular aldolase mimics have been constructed. Gellman, Hilvert, and co-workers designed a robust catalytic foldamer (Figure 2A), which utilized *trans*-2-aminocyclohexanecarboxylic acid-based scaffold and contained plentiful β^3-homolysine (β^3-hLys) residues.[40] The clustering of β^3-hLys residues decreased the side-chain ammonium pK_a values and facilitated the amine-catalyzed retro-aldol cleavage of β-hydroxyketone to generate pyruvate and benzaldehyde. The catalytic reaction followed Michaelis-Menten kinetics, and the activities conformed well to the computationally designed retro-aldol enzymes.[43]

Besides Lys, the proline (Pro) that is capable of forming enamine intermediate with the carbonyl group of substrates is frequently incorporated into the peptide-based aldolase mimics as well. Escuder, Miravet, and co-workers developed an L-Pro-based supramolecular gel (Figure 2B), which could work as a basic

Table 1. The kinetic parameters of the aldolase mimics

Catalyst	Substrate	k_{cat} (min^{-1})	k_{cat}/K_m (M^{-1} min^{-1})	Reference
β^3-homolysine foldamer	β-Hydroxyketone	0.13	26.0	Müller et al.[40]
C_{10}-FFVK nanotube/Fmoc-Y	Methodol	4.93×10^{-3}		Reja et al.[42]
Ac-KLVFFAL-NH_2	*R*-methodol	2.45×10^{-3}		Omosun et al.[46]
Ac-KLVFFAL-NH_2	*S*-methodol	3.72×10^{-3}		Omosun et et al.[46]

catalyst at 5°C for the Henry nitroaldol reaction between nitroalkane solvent (nitroethane or nitromethane) and benzaldehyde derivative (4-chlorobenzaldehyde or 4-nitrobenzaldehyde).[41] During the reaction process, the gelatinous catalyst adopted an ionic pair mechanism which was caused by nitroalkane deprotonation. The catalytic activity of the gel was attributed to the basicity boost of L-Pro residues as a result of gelation. This was the first time that the gel phase served as an active phase. When the temperature rose from 5°C to 25°C, the gel was transformed into a solution, accompanied by dramatic decrease of aldol conversion and increase of reaction pathway leading to alkenes via iminium intermediates. In this research, the amino acids played both structural and catalytic roles, which may shed light on the origin of life.

Wennemers and co-workers made use of a self-assembled amphiphilic tripeptide (H-$_D$-Pro-Pro-Glu-NH-$C_{12}H_{25}$) to catalyze asymmetric conjugate addition reactions of aldehydes to nitroolefins in water with high stereoselectivity (ee: up to 91%) and yields (above 95%).[44] Compared to the relatively low catalytic stereoselectivity (ee: 73%) and yields (28%) of its parent tripeptide (H-$_D$-Pro-Pro-Glu-NH_2) system, this peptide exhibited the importance of interior hydrophobic microenvironment to the efficient catalysis, like the hydrophobic pockets of the enzymatic active sites. This research gave interesting enlightenment that hydrophobic compartments containing catalytically active residues may have played a critical role in the early evolution of natural enzymes. Ashkenasy, Escuder, and co-workers reported aldolase-mimicking catalytic hydrogels formed by amphiphilic $P(FE)_n$ or $P(EF)_n$ short peptides with C-terminal long alkyl chains.[45] The alkyl chains were designed to form hydrophobic regions which could facilitate the solubilization of hydrophobic substrates. The obtained hydrogels catalyzed aldol reaction between cyclohexanone and 4-nitrobenzaldehyde in high efficiency (yields increased from 14% to over 99%) and stereo-selectivity (d.r. *syn*/*anti* were between 10 : 90 and 20 : 80). Catalytic kinetics of this system did not conform to the classical Michaelis-Menten model, indicating nonspecific substrate binding but just preferential gathering of substrates within the hydrophobic regions.

In a significant development, Das and co-workers constructed an amyloid-like nanotube that was capable of catalyzing both the retro-aldol and forward aldol reactions.[42] They used an amphiphile peptide C_{10}-FFVK to assemble into the nanotube with exposed Lys residues, which showed obvious catalytic activity toward the retro-aldol reaction of methodol to 6-methoxy-2-naphthaldehyde (6-MND) (Figure 2C). Inspired by the cooperative catalytic function of adjacent Lys and Tyr residues in natural aldolases, they incubated the Fmoc-Tyr with self-assembled C_{10}-FFVK nanotube. Fmoc-Tyr molecules could adhere to the amyloid-like nanotube through hydrophobic interactions, resulting in the high-density array of proximal Lys and Tyr residues on its surface. Noncovalently bound Fmoc-Tyr enhanced the catalytic retro-aldol activities toward methodol 4.9 times higher than that of the nanotube without Fmoc-Tyr. Moreover, the authors demonstrated that, with the assistance of Fmoc-Tyr, the amyloid-like nanotube was able to catalyze cascade retro-aldol and forward aldol reactions in the presence of methodol and different nucleophilic ketones. This was the first reported peptide-based artificial enzyme that could catalyze a cascade reaction involving both the cleavage and formation of C-C bonds.

The kinetic parameters of the aldolase mimics are listed in Table 1. In addition to the most common Lys and Pro, other types of amino acids, such as arginine (Arg), phenylalanine (Phe), and glutamine (Gln), were also used solely or associatively to construct the active sites of aldolase-mimicking artificial enzymes.[47,48]

Laccases

Laccases are a typical family of copper-dependent oxidase, which employ the oxygen as electron acceptor to oxidize diverse organic substrates,[49,50] particularly the aromatic compounds, such as phenol, bisphenol A, or azo dyes. Therefore, laccases have always been considered as green catalysts and are widely applied in degrading organic pollutants. As a multi-copper oxidase, the active site of laccase possesses four copper

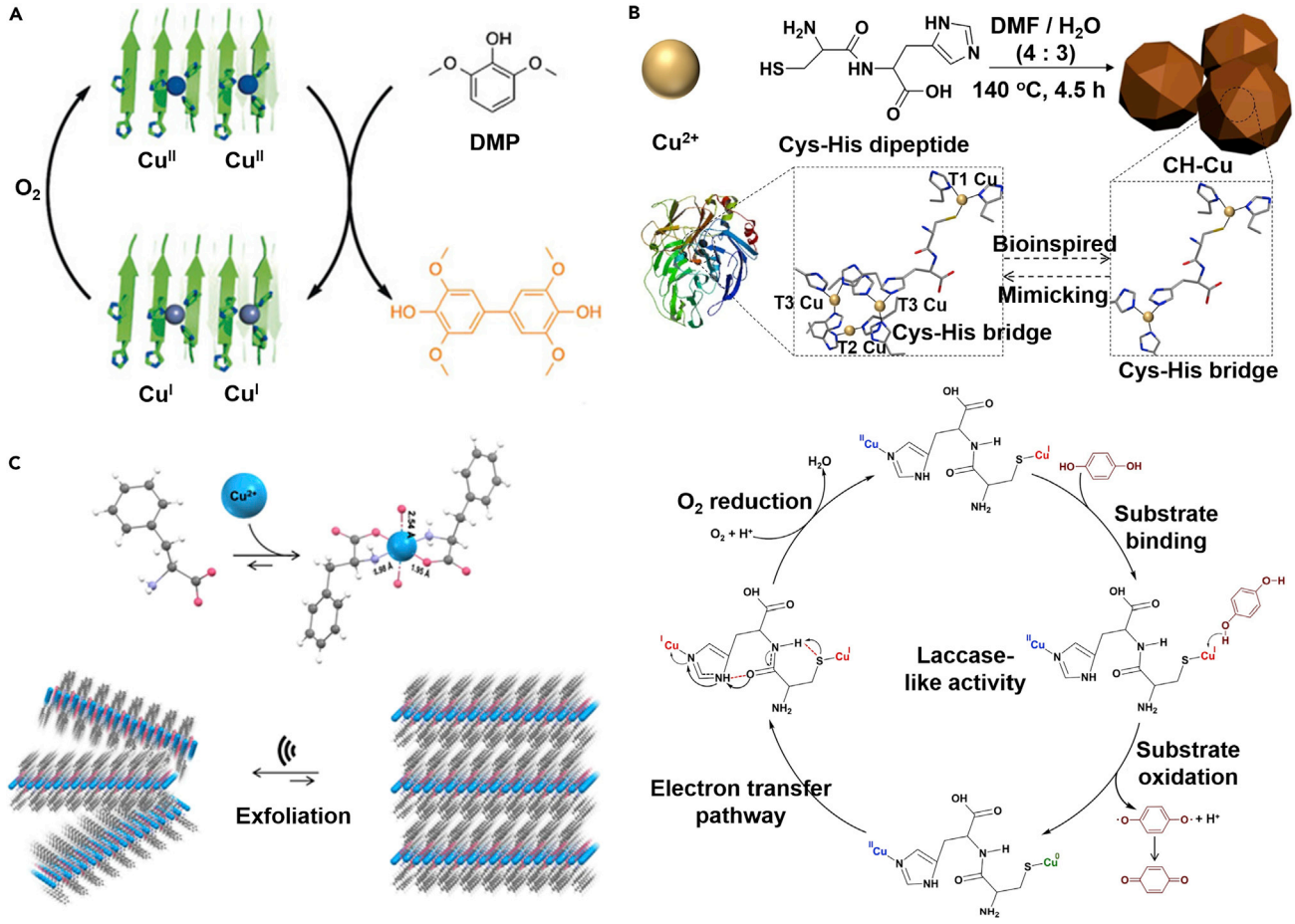

Figure 3. Representative peptide-based supramolecular laccase mimics

(A) Copper-containing amyloid-like fibrils for DMP oxidation in the presence of oxygen. Reproduced with permission from ref.,[54] copyright 2016, John Wiley & Sons, Inc..

(B) Peptide-based laccase-mimicking artificial enzyme prepared through hydrothermal process and the catalytic mechanism. Reproduced with permission from ref.,[55] copyright 2019, Elsevier B.V..

(C) laccase-mimicking layered van der Waals crystals prepared by co-assembly of Phe and copper (II) ions. Reproduced with permission from ref.,[56] copyright 2022, Springer Nature.

ions, which are distributed in three types of binding sites termed Type I, Type II, and Type III.[51] Among them, Type I and Type II are both mononuclear and paramagnetic, while Type III is binuclear and antimagnetic. In the Type I binding site, copper ion is usually coordinated to two histidine (His) residues and one Cys residue. In some laccases from specific bacteria and plants, there is an additional weak coordinate bond between the Type I copper and a neighboring methionine (Met) residue.[52,53] In the Type II binding site, the coordination sphere of copper ion contains two His residues and one water molecule. The Type III binding site is binuclear, in which two copper ions are bridged through a hydroxide bridge, and each copper ion is coordinated with three His residues. The Type II and Type III binding sites form a triangular trinuclear copper cluster. The Type I copper ion accepts an electron from the reducing substrate and transfers the electron to the trinuclear copper cluster comprising Type II and Type III binding site, which then binds and reduces the oxygen to water. The catalytic activities of natural laccases rely on the spatial distribution of copper ions and their ligands. Emulating the chemical structures of copper binding sites in natural laccases is the key to design peptide-based supramolecular laccase mimics.

Korendovych and co-workers *de novo* designed a library of short peptides containing alternate His residues (Figure 3A), which could self-assemble with copper ions to catalyze the oxidative dimerization of 2,6-dimethoxyphenol (DMP) using oxygen as an oxidant.[54] After experimentally screening, they found the heptapeptide Ac-IHIHIQI-NH_2 displayed the highest catalytic activity, accompanied by the strongest

Table 2. The kinetic parameters of the laccase mimics

Catalyst	Substrate	k_{cat} (s^{-1})	k_{cat}/K_m (M^{-1} s^{-1})	Reference
Ac-IHIHIQI-NH_2/Cu^{2+}	DMP	6.6×10^{-3}	31	Makhlynets et al.[54]
CH-Cu	2,4-DP + 4-AP	3.18×10^{2}	7.58×10^{2}	Wang et al.[55]
CA-Cu	2,4-DP + 4-AP	4.41×10^{2}	3.68×10^{3}	Xu et al.[59]
Phe/Cu^{2+}	2,4-DP + 4-AP	11.9	62.65	Makam et al.[56]

tendency to form β-sheet secondary structures and amyloid-like fibrils. The catalytic performance was calculated to be 65-fold higher than that of free copper ions in buffer. In comparison, the non-fibril-forming control peptide NH_2-IHIHIQI-COOH (the same sequence but uncapped) exhibited lower catalytic activity than that of blank control group. The low-temperature EPR (electron paramagnetic resonance) measurement proved the coordination sphere of copper ions bound to the most active heptapeptide was akin to that in the Type II binding site of laccase. This research reported the first catalytic amyloid that was capable of fostering redox-mediated chemical reaction, which supported the amyloid-first hypothesis of enzymes evolution.[57,58]

Given the fact that the copper ions in natural laccases are mainly coordinated with His and Cys, Huang, Qi, and co-workers hydrothermally synthesized a laccase-mimicking artificial enzyme employing self-assembled Cys-His dipeptide and copper chloride as precursors.[55] The chromogenic reaction between 4-aminoantipyrine (4-AP) and 2,4-dichlorophenol (2,4-DP) was used to evaluate the catalytic property of the nanocatalyst (Figure 3B). In comparison with laccase, this artificial enzyme showed higher catalytic activity at the same mass concentration and better tolerance to diverse harsh conditions, such as extreme pH (pH 3-9), high salinity (500 mM NaCl), and high temperature (up to 120°C). They also fabricated another laccase-mimicking artificial enzyme through the similar synthetic method but used Cys-Asp instead of Cys-His as the dipeptide precursor.[59] The resultant Cys-Asp-based artificial enzyme displayed higher catalytic performance than that prepared using Cys-His dipeptide.

Recently, a minimalist strategy was employed to construct supramolecular laccase mimics by taking advantage of single amino acid molecules instead of the peptides. Makam, Gazit, and co-workers demonstrated the self-assembled layered van der Waals crystals (Figure 3C), which were composed of single Phe and copper (II) ions, possessed laccase-like activities[56] toward catalyzing oxidation of 2,4-DP. *In-situ* Raman measurements and computational studies demonstrated the transfer of H atom to the carboxylate (-COO) group of F-Cu was the crucial step of the catalytic process. Moreover, the self-assembled amino acid crystals showed stability against extreme environment, such as extreme pH, high ionic strength, long storage time, and high temperature, and were more recyclable than the laccase. The authors claimed that this research might supplement a missing link in seeking the prebiotic catalysts.

The kinetic parameters of the laccase mimics are listed in Table 2.

Peroxidases

Peroxidases can catalyze the oxidation reactions between the peroxides and the reducing substrates.[60] A large proportion of peroxidases are essentially the proteinaceous enzymes employing heme as cofactor, for instance, horseradish peroxidase (HRP), cytochrome *c* peroxidase (CCP), and lactoperoxidase (LPO). The active site of peroxidase normally consists of one heme cofactor (a few peroxidases contain two heme cofactors in the active site, such as the di-haem cytochrome *c* peroxidase[61]) and some reactive residues around heme. Taking HRP as the example, in its active site, the cofactor heme is coordinated with a proximal His residue (His170), and the His42 and Arg38 residues are located on the distal side of heme.[62] These three residues act synergistically to promote activation of heme and formation of the intermediate compound I. On account of the hydrophobic pocket afforded by the residues around heme (Phe, His, Gly, Pro, etc.), HRP utilizes a lot of aromatic compounds as reducing substrates. Inspired by the chemical structures of active sites in natural peroxidases, a variety of peptide-based peroxidase-mimicking artificial enzymes have been constructed.

Chang, Xu, and co-workers fabricated a hemin-containing hydrogel by the co-assembly of hemin, Fmoc-Phe, and Fmoc-Lys.[63] This hydrogel was able to catalyze the oxidation of pyrogallol to purpurogallin in

both water and toluene. After introducing unmodified His as the fourth constituent, the peroxidase-like catalytic activity of the hydrogel was further improved. The highest catalytic efficiency, about 60% of the initial activity of HRP in water, was achieved using toluene as solvent. The authors proposed that the catalytic activities of such hydrogels emanated from the localization of hemin, which protected it from dimerization and oxidative degradation. In a subsequent research, they prepared a similar hydrogel utilizing Fmoc-Phe, Fmoc-Lys, and a chemically modified hemin as gelators.[64] The consequent supramolecular hydrogel also showed the highest catalytic efficiency in toluene, which reached approximately 90% of the initial activity of HRP in water.

Bhattacharjya and co-workers reported two kinds of β-hairpin peptides, named IV8 and IV8FA, could display peroxidase-like activity after binding heme in the micellar environment.[65] Both the peptides contained myristyl chain for membrane anchoring, ^{D}P-G segment for nucleation of type I′ or type II′ β-turn, His residue for heme binding, and tryptophan (Trp) residue for anchoring peptide into the water-lipid interface. The catalytic activities of the self-assembled entities toward 3,3′,5,5′-tetramethylbenzidine (TMB) oxidation were comparable to that of ME1 protein and protein 86. In a further study, this group designed a series of four-stranded β-sheet miniproteins containing heme cofactors.[66] Owing to introduction of bis-histidine ligands and creation of the hydrophobic binding pocket, the optimized heme-binding affinity of these miniproteins was comparable to that of natural hemeproteins. These miniproteins showed the high stability against high temperature and denaturant, while their peroxidase-mimicking activities did not increase with higher heme-binding affinity.

In view of the coordinate bond between heme and His residue in the active site of HRP, Zou, Yan, and co-workers constructed the amino acid-based peroxidase-mimicking nanozymes (adjustable diameter range: 50–120 nm) through co-assembly of Fmoc-His (FH) and hemin.[67] The morphologies and structures of the nanozymes, as well as the resultant peroxidase-like catalytic activities, could be tailored by changing the molar ratio of FH to hemin (Figure 4A). Notably, the optimum catalytic performance (FH/hemin = 4 : 1) of the nanozyme (k_{cat}/K_m/M = 1.33 $(gL^{-1})^{-1}s^{-1}$) was comparable to that of HRP (k_{cat}/K_m/M = 1.73 $(gL^{-1})^{-1}s^{-1}$).

Instead of heme, Wang, Qi, and co-workers employed ferrocene (Fc) as prosthetic group to construct peptide-based peroxidase-mimicking artificial enzyme.[70] The artificial enzyme was prepared by self-assembly of ferrocene-modified tripeptide (ferrocenyl-Phe-Phe-X), in which the X referred to Phe, Asp, His, or Arg. Through adjusting the type of X residue, the morphologies and catalytic activities of the artificial enzymes varied. When using Phe or Asp as the third residue, nanofibers with low peroxidase-like performance were obtained. Nevertheless, when using His or Arg, nanospheres with high catalytic activities were observed. His and Arg are exactly the essential residues in the active site of HRP. The generation of hydroxyl radicals (•OH) intermediate was observed during the catalytic process, and the steady-state kinetics analysis demonstrated that this ferrocene-based catalytic system followed a ping-pong multiple substrate mechanism. That meant the artificial enzyme first reacted with one H_2O_2 to generate an •OH intermediate, and then the •OH reacted with the reductive substrate TMB.

Peptoids, or poly-N-substituted glycines, have tailorable side chains and greater stabilities over the peptides. Most recently, Zhang and co-workers assembled the designed peptoids with hemin into crystalline tubular peroxidase mimetics.[68] The chemical composition of the active sites and the catalytic properties of these peroxidase mimetics were modulated by altering the terminal ligands and side-chain groups of the peptoids (Figure 4B). A peptoid-based mimic containing N-(2-carboxyethyl)glycine terminal ligands and pyridyl side chains showed the highest catalytic activities, with the V_{max}/K_m value toward TMB oxidation reaching $5.81 \times 10^{-3}\ s^{-1}$. Kinetic analysis indicated the catalytic reaction followed a ping-pong mechanism, in which H_2O_2 and the reducing substrate bound to the metal center sequentially. The H_2O_2 oxidized the hemin to generate the compound I, which accepted the electrons from the reducing substrate for the oxidation. This peptoid-based mimic efficiently catalyzed the depolymerization of a biomass substrate, organosolv lignin, under mild conditions, in the presence of H_2O_2. These peroxidase mimetics also displayed improved initial catalytic velocity at high temperature (up to 90°C), indicating their robust catalytic properties.

In addition to the heme-dependent peroxidase-mimicking catalysts, many efforts have been made to explore the fabrication of cofactor-free peroxidase mimics, which helps understand the early evolutionary pathway of natural enzymes. Very recently, we reported a heme-free peptide-based peroxidase-mimicking catalytic

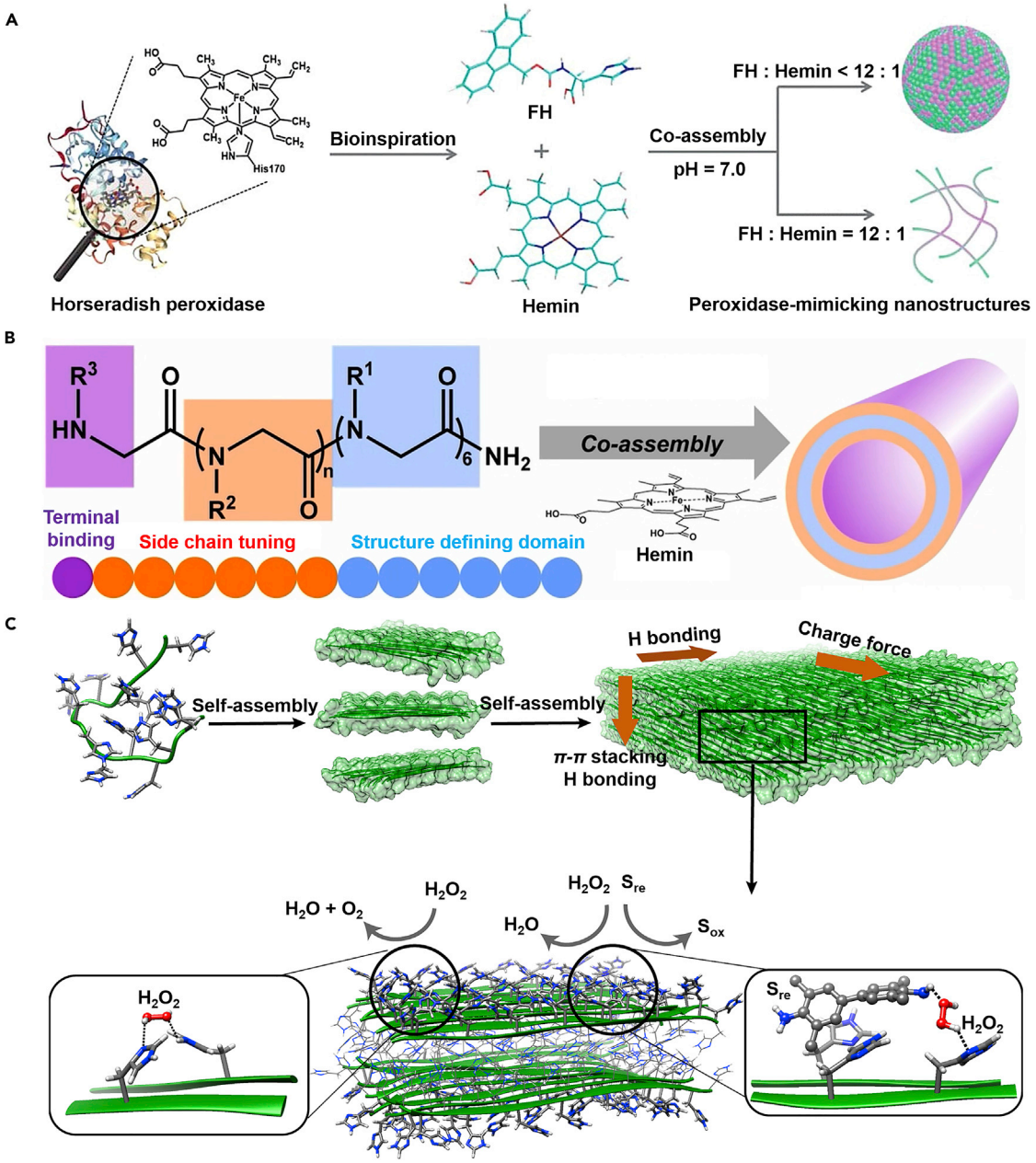

Figure 4. Representative peptide-based supramolecular peroxidase mimics

(A) Peroxidase-mimicking nanostructures prepared by co-assembly of FH and hemin, with molar ratio-dependent morphology. Reproduced with permission from ref.,[67] copyright 2021, John Wiley & Sons, Inc..

(B) Molecular representation of peptoid sequence and its co-assembly with hemin into crystalline tubular peroxidase mimetic. Reproduced with permission from ref.,[68] copyright 2022, Springer Nature.

(C) Hierarchical self-assembly of oligohistidines into planar crystal nanostructures with peroxidase-like catalytic activities. Reproduced with permission from ref.,[69] copyright 2021, Springer Nature.

system.[69] We constructed a series of supramolecular artificial enzymes using oligohistidines of different lengths (as short as dipeptide). The self-assembled cofactor-free artificial enzymes exhibited crystal-like lattices composed of β-sheet secondary structures and peroxidase-like catalytic activities in the oxidation of various reducing substrates (TMB, NADH, or homovanillic acid [HVA]) by H_2O_2 (Figure 4C). Catalysis kinetics, EPR, and quantum chemical calculations results showed the simultaneous adsorption of TMB and H_2O_2 to the catalyst on its facet (010). The formation of ternary complex reactive intermediate was a key event leading to

Table 3. The kinetic parameters of the peroxidase mimics

Catalyst	Substrate	k_{cat} (s^{-1})	k_{cat}/K_m (M^{-1} s^{-1})	Reference
hemin(Phe + His)	Pyrogallol	17.42		Wang et al.[63]
Gel-6	Pyrogallol	25.95		Wang et al.[64]
Peptide 4	ABTS	295.88	2.75×10^3	D'Souza et al.[66]
FH: Hemin = 4 : 1	TMB	0.160	2918	Geng et al.[67]
Fc-FFR NSs	TMB	3.4×10^{-3}	23.42	Feng et al.[70]
H15	TMB	1.322×10^{-4}	0.704	Liu et al.[69]
Ac-VHVHVQV-NH_2	OPD	1.9×10^{-4}	0.45	Zozulia et al.[71]
H5-SG4-Q11	TMB	1.038×10^{-3}	2.91	Liu et al.[72]

the subsequent catalytic reactions. Notably, the cofactor-free artificial enzymes could be switched between active and inactive states after cycled thermal or acid treatment, implying the reversible assembly and disassembly of the active sites. After ten or more cycles, the catalytic performance was recovered, demonstrating the robustness of the cofactor-free artificial enzymes. These findings provided a possible model for primitive enzymes and may explain how the early biocatalysts survived under prebiotic conditions. Korendovych and co-workers reported the self-assembled peptide (Ac-VHVHVQV-NH_2) also displayed peroxidase-like activity in the absence of any cofactor.[71] They speculated such catalytic activity may stem from the change in redox potential of the substrate after adsorption to the self-assembled peptides. In a further research, we assembled a His-rich pentapeptide (NH_2-HHHHH-COOH) into amyloid-like structures by conjugating the oligohistidine segment to a fibril-forming peptide (NH_2-QQKFQFQFEQQ-$CONH_2$).[72] The amyloid-like structures possessed one order higher catalytic efficiency than the oligohistidine assembly. The kinetic parameters of the peroxidase mimics are listed in Table 3. Besides the peptide-based cofactor-free peroxidase mimics, we have also designed other peroxidase-mimicking artificial enzymes through the co-assembly of peptides, DNA, and hemin.[73–77] In these supramolecular systems, we demonstrated remarkable synergistic effects of peptide and DNA in the enhancement of the catalytic activities.

Hydrolases

Hydrolases are hydrolytic enzymes that break some specific chemical bonds with water, resulting in the disintegration of large molecules into small pieces. Typical hydrolases in nature include esterases, phosphatases, proteases, etc. Most natural hydrolases included at least one His residue in the active site, which assists in abstracting proton from the water to enhance nucleophilic reactivity of the remaining anion. This His residue is also allied with other residues to form a catalytic dyad (e.g., Cys-His[78] and Asp-His[79]) or triad (e.g., Ser-His-Asp[80] and Cys-His-Asp[81]), or in some cases, allies itself with two other His residues to coordinate with metallic ion as cofactor (e.g. Zn^{2+}).[82,83] Numerous efforts have been made through peptide self-assembly to reconstruct the active sites of hydrolases for the catalytic properties.

In a pioneering research, Stupp and co-workers synthesized a peptide amphiphile that consisted of a short peptide sequence (including two His residues) and a palmitoyl group.[84] This peptide amphiphile self-assembled into ordered nanofibers with high aspect ratio and exposed His residues on the surface. This catalyst exhibited considerable esterase-like activity in the hydrolysis reaction of 2,4-dinitrophenyl acetate (DNPA). The control samples that contained two His residues but only formed less ordered spherical aggregates showed lower hydrolysis rates.

Inspired by the fact that many natural hydrolases employ Zn^{2+} ion as cofactor, De-Grado, Korendovych, and co-workers designed a series of amyloid-forming heptapeptides containing two separate His residues and alternating hydrophobic residues.[85] The His residues bound the Zn^{2+} ion which helped stabilize the amyloidal structures and also served as cofactor to catalyze hydrolysis reactions. In the presence of Zn^{2+} ions, amyloidal nanofibrils with β-sheet secondary structures were formed through self-assembly (Figure 5A). With *p*-nitrophenyl acetate (*p*-NPA) as the chromogenic substrate, they investigated the esterase-like catalytic activities of the self-assembled nanofibrils formed by divergent peptide sequences. The Ac-IHIHIQI-$CONH_2$ sequence was found to be the most active, possessing hydrolytic efficiency rivalling that of natural carbonic anhydrase by weight. These results indicated the catalytic amyloids might be the intermediates in evolutionary journey of contemporary esterases. In another study, Serpell and co-workers found both the

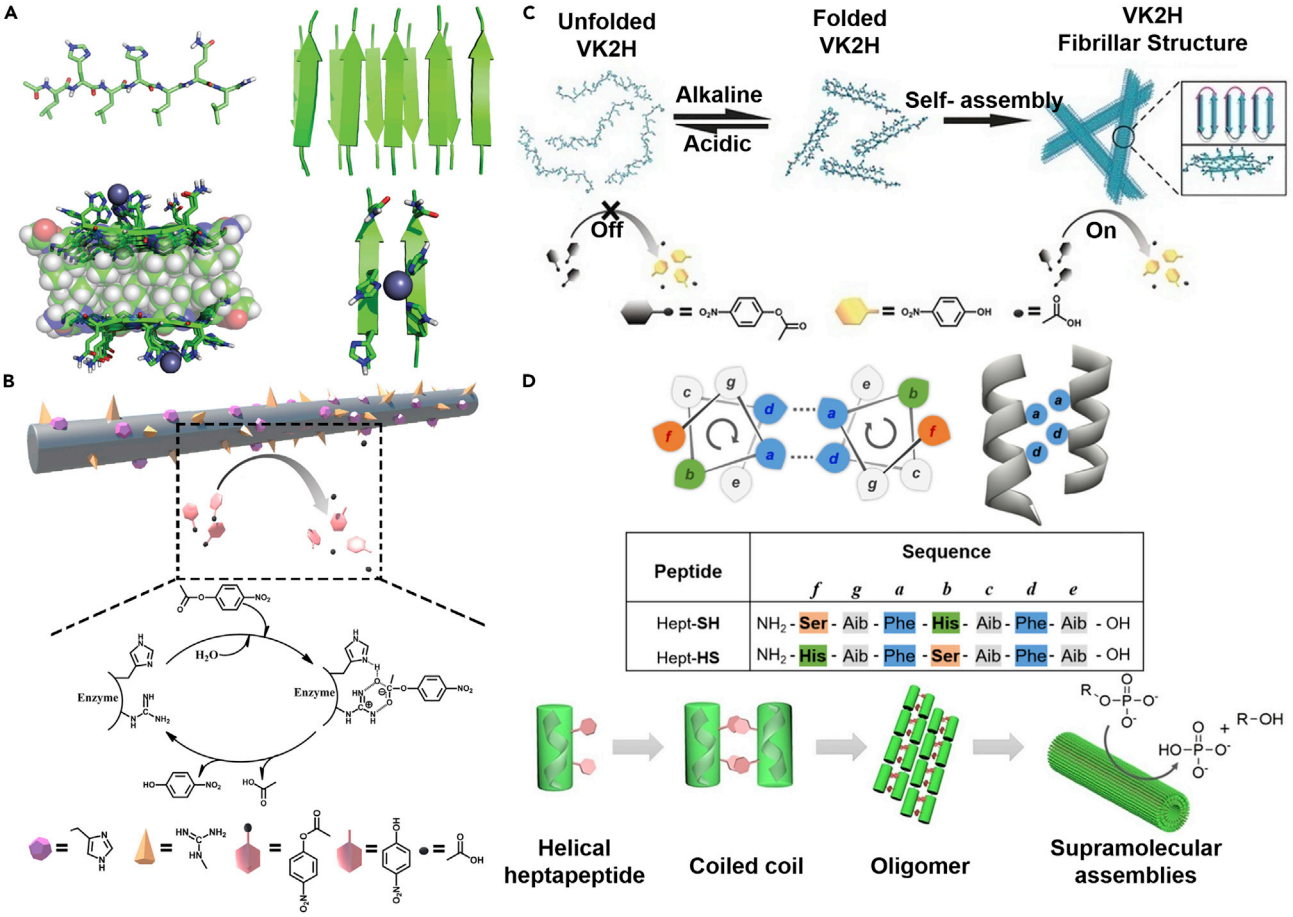

Figure 5. Representative peptide-based supramolecular hydrolase mimics

(A) Computationally simulated models of the amyloidal structures consisting of Ac-IHIHIQI-$CONH_2$ peptide and Zn^{2+} ions. Reproduced with permission from ref.,[85] copyright 2014, Springer Nature.

(B) Probable catalytic mechanism for the hydrolysis of *p*-NPA with the assistance of co-assembled Q11H/Q11R nanofibrils. Reproduced with permission from ref.,[86] copyright 2014, American Chemical Society.

(C) Schematic illustration of the pH responsivity of hydrolase mimic based on the conformation change of VK2H peptide. Reproduced with permission from ref. [87], copyright 2017, John Wiley & Sons, Inc.

(D) Design principle of the helical heptapeptides and the process of their hierarchical self-assembly into fibrillar nanostructures with phosphatase-like catalytic activity. Reproduced with permission from ref.,[88] copyright 2021, American Chemical Society.

binding of Zn^{2+} ions and the periodic assembly of peptides were crucial to the catalytic activities of esterase-mimicking amyloids.[89]

The co-assembling peptides with different sequences have also been utilized to construct hydrolase-mimicking artificial enzymes. In a typical research, Liu, Liang, and co-workers synthesized two kinds of peptides, the Q11H (NH_2-HSGQQKFQFQFEQQ-Am) and Q11R (NH_2-RSGQQKFQFQFEQQ-Am), by modifying the fibril-forming Q11 peptide (QQKFQFQFEQQ) with a His and an Arg at the terminal, respectively (SG was used as spacer).[86] They observed the esterase-like activity of the nanofibrils formed by co-assembling Q11H and Q11R was higher than that of the nanofibrils assembled from Q11H or Q11R. The higher catalytic performance of the co-assembled system was dependent on the cooperation between the imidazolyl group of His residue and the guanidyl group of Arg residue. The latter favored stabilization of the transition state of substrate by binding the oxide ions of intermediate complex, as well as assisted in cleavage of the C-O bond to release product and recover the active site (Figure 5B).

Through introducing stimuli-response units to the peptides, the structures and catalytic activities of the artificial enzymes can be dynamically regulated by external triggers, such as pH and light. Ulijn and

co-workers constructed a pH-responsive esterase mimic based on peptide self-assembly.[87] They synthesized a peptide, VK2H, composed of a His residue, a flexible spacer SG, and two pH-responsive segments of Val-Lys repeats linked via a ^{D}PPT turn sequence (Figure 5C). With the pH changed from 6.0 to 9.0, the secondary structures of VK2H peptides were transformed from random coils to β-sheets. This resulted in the rearrangement of His residues from unordered to well-ordered distribution, and accordingly, the transition of this esterase mimic from catalytically inactive to active state. Such changes were reversible. Wang, Qi, and co-workers fabricated a peptide-based light-switchable esterase mimic through covalently modifying a tripeptide (GFG) with light-responsive azobenzene (Azo) group and catalytic His residue at its N- and C-terminus, respectively.[90] The Azo-GFGH peptides self-assembled into regular nanofibers under visible light, which led to the close-packed array of the peptides and basicity enhancement of the His residues exposed on the surface. This lowered the pK_a of H_2O and stabilized the remaining anions for nucleophilic attack on the *p*-NPA substrates. Moreover, the hydrophobic microenvironment that stemmed from azobenzene and phenylalanine molecules enhanced the interaction between *p*-NPA and the active sites, which accelerated the catalytic process. However, after UV irradiation, the nanofibers partially disassembled into amorphous aggregates because of the *trans*- to *cis*-isomerization of Azo, accompanied by a decline in catalytic efficiency. Such morphological and catalytically active changes were fully reversible.

Inspired by the Ser-His-Asp catalytic triad in hydrolases, Qi and co-workers co-assembled the Fmoc-FFS, Fmoc-FFH, and Fmoc-FFD peptides into nanofibers.[91] At an optimal ratio of 1 : 40: 1 (Fmoc-FFS/Fmoc-FFH/Fmoc-FFD), the co-assembled nanofibers displayed the highest catalytic performance in hydrolysis of *p*-NPA, which was approximately 2-fold of that of the assembly made up of Fmoc-FFH. Moreover, after molecular imprinting using the *p*-NPA as template, the optimal catalytic performance could be further enhanced by 7.86 times. In another research, Guler and co-workers reconstructed the S/H/D catalytic triad by the co-assembly of three types of lipopeptides that contained the key residues (Ser, His, and Asp).[92] The resultant co-assembly also showed significant synergy between the three key residues in enhancing hydrolysis of *p*-NPA or acetylthiocholine.

Das and co-workers reported an amyloid nanotube formed by Im-KLVFFAL-NH_2 peptide (Im-KL).[93] The self-assembled nanotube catalyzed hydrolysis of ester substrates by virtue of the formation of reversible covalent bonds. In the elaborately designed peptide sequence, the terminal-adjacent Lys residue and imidazole group were exposed on the surface of nanotube upon self-assembly. The Lys residue assisted in anchoring substrate via formation of a Schiff imine, and the imidazole group hydrolyzed the ester bond of the substrate. Replacement of the Lys residue with Arg, ornithine, or Glu resulted in dramatic decrease in esterase-like catalytic activities of the self-assembled nanotube.

A few studies about peptide-based phosphatase mimics have also been reported. Razkin, Baltzer, and co-workers developed a helix-loop-helix motif folded by a 42-residue peptide, which self-dimerized to turn into a four-helix bundle.[94] The four-helix bundle exposed active site composed of two His and four Arg residues on its surface and exhibited the ability to catalyze hydrolysis reaction of phosphodiesters. Employing uridine 3′-2,2,2-chloroethyl phosphate, a mimic of RNA, as substrate, the second order rate constant was more than two orders of magnitude larger than that of the reaction catalyzed by imidazole groups alone. Subsequently, they introduced two Tyr residues into the active site to make the His residues flanked by Arg and Tyr residues, resulting in further improvement of the phosphatase-like catalytic activities.[95]

Considering that the catalytic activity of alkaline phosphatase (ALP) arose from the imidazole groups of His residues in the active sites,[96] Tekinay, Guler, and co-workers synthesized a peptide amphiphile (Lauryl-VVAGHH-Am) that was able to self-assemble into nanofibers with high-density His residues at the periphery.[97] The nanofibers showed significant phosphatase-like catalytic activities using the *p*-nitrophenyl phosphate (*p*-NPP) as substrate. The nanofibers also promoted the hydrolysis of β-glycerophosphate (β-gly) to inorganic phosphate for CaP mineralization and served as bone-like nodule inducing scaffold to induce *in vitro* osteogenic differentiation.

By emulating the α-helix structures in the catalytic domain of metal-free natural phosphatase, Wang, Qi, and co-workers designed a helical heptapeptide (Hept-SH) consisting of two hydrophobic Phe residues, three non-coded α-aminoisobutyric acid (Aib) residues, one Ser residue, and one His residue.[88] This Hept-SH heptapeptide self-assembled into fibrillar nanostructures, which displayed markable catalytic activities in the hydrolysis

Table 4. The kinetic parameters of the hydrolase mimics

Catalyst	Substrate	k_{cat} (s^{-1})	k_{cat}/K_m (M^{-1} s^{-1})	Reference
Peptide amphiphile	DNPA	1.67×10^{-2}	19.76	Guler et al.[84]
Ac-IHIHIQI-$CONH_2/Zn^{2+}$	*p*-NPA	2.6×10^{-2}	62 ± 2	Rufo et al.[85]
Ac-IHIHIYI-NH_2/Zn^{2+}	*p*-NPA	8.26×10^{-3}	355.00	Al-Garawi et al.[89]
$Q11HR_{max}$	*p*-NPA	2.64×10^{-3}	0.15	Zhang et al.[86]
VK2H	*p*-NPA	0.07	19.18	Zhang et al.[87]
Azo-GFGH (Before UV)	*p*-NPA	3.67×10^{-3}	0.23	Zhao et al.[90]
Azo-GFGH (After UV)	*p*-NPA	3.00×10^{-3}	0.18	Zhao et al.[90]
$CoA\text{-}HSD_{max}$	*p*-NPA	3.00×10^{-2}	1.86×10^{-1}	et al.[91]
D/H/S	*p*-NPA	4.41×10^{-3}	126.62	Wang et al.[92]
Im-KLVFFAL-NH_2	*p*-NPA		2.4	Sarkhel et al.[93]
Lauryl-VVAGHH-Am	*p*-NPP	1.83×10^{-5}	0.69	Gulseren et al.[97]
Hept-SH	*p*-NPP	18.33×10^{-5}	0.70	Wang et al.[88]
Hept-SH	*p*-NPA	2.40×10^{-2}	1.07	Wang et al[88]
1_{TB}	*p*-NPA	1.07×10^{-3}	1.71	Singh et al.[98]
Phe/Zn^{2+}	*p*-NPA		76.54	Makam et al.[100]
HY9	*p*-NPA	0.35×10^{-2}	1.64	Díaz-Caballero et al.[101]
7IY	Paraoxon	8.0×10^{-5}	2.83×10^{-2}	Lengyel et al.[102]
Aβ42 fibrils	*p*-NPA	1.89×10^{-3}	0.64	Arad et al.[103]

of *p*-NPP (Figure 5D). Density functional theory (DFT) calculation indicated the phosphatase-like activity was derived from the helical dipole moment, which favored the substrate binding. Molecular docking (MD) and filtration/sedimentation experiments revealed the significance of peptide self-assembly to the formation of active sites. Furthermore, this peptide-based phosphatase mimic could substitute for some natural phosphatases in specific physiological functions, such as ATPase in an ATP cleavage reaction and ALPase in a calcium-deposition process. This metal-free phosphatase mimic may provide a probable model for the helical peptide-based primitive enzymes.

Recently, by incorporating the similar amyloid-forming peptide fragment (VFFA), Pal and co-workers designed two kinds of peptide amphiphiles (Fmoc-VFFAHH and Cou-VFFAHH).[98] The His residues at C-terminal served as active sites for catalyzing the hydrolysis reactions, and the Fmoc- and Cou- groups at N-terminal were used as stimuli-response units. Both peptide amphiphiles exhibited pathway-driven self-assembly behaviors to form diverse nanostructures, which were interconvertible via external stimuli such as heat, light, and chemical cues, leading to tailorable esterase-like catalytic activities toward *p*-NPA hydrolysis. The same group also demonstrated chirality-driven self-sorting of the VFFA fragment and seed-promoted elongation of homochiral nanofibers from enantiomeric peptide amphiphiles (C_{10}-$L/_D$-VFFAKK).[99] This provided the possibility of constructing peptide-based supramolecular active sites with chiral configuration, which might display high catalytic stereo-selectivity.

The kinetic parameters of the hydrolase mimics are listed in Table 4.

MULTIFUNCTIONAL PEPTIDE-BASED SUPRAMOLECULAR CATALYSTS

It is believed that primitive enzymes could catalyze a wide range of biochemical transformations to establish the protometabolic reaction networks, and the substrate specificity of modern enzymes is a result of long-term natural evolution and selection.[104–106] However, it is difficult to identify the evolutionary pathways from promiscuous primitive enzymes to functionally specific extant enzymes. Constructing the peptide-based artificial enzymes with multi-specificity toward substrate may provide some clues. In recent years, many multifunctional supramolecular catalysts that were able to catalyze orthogonal or cascade reactions have been fabricated by means of peptide self-assembly.

Lynn and co-workers designed a short peptide K1 (Ac-KLVFFAL-NH_2) based on the nucleating core sequence (LVFF) of Amyloid-β (Aβ) peptide.[46] This K1 peptide can self-assemble at neutral pH into

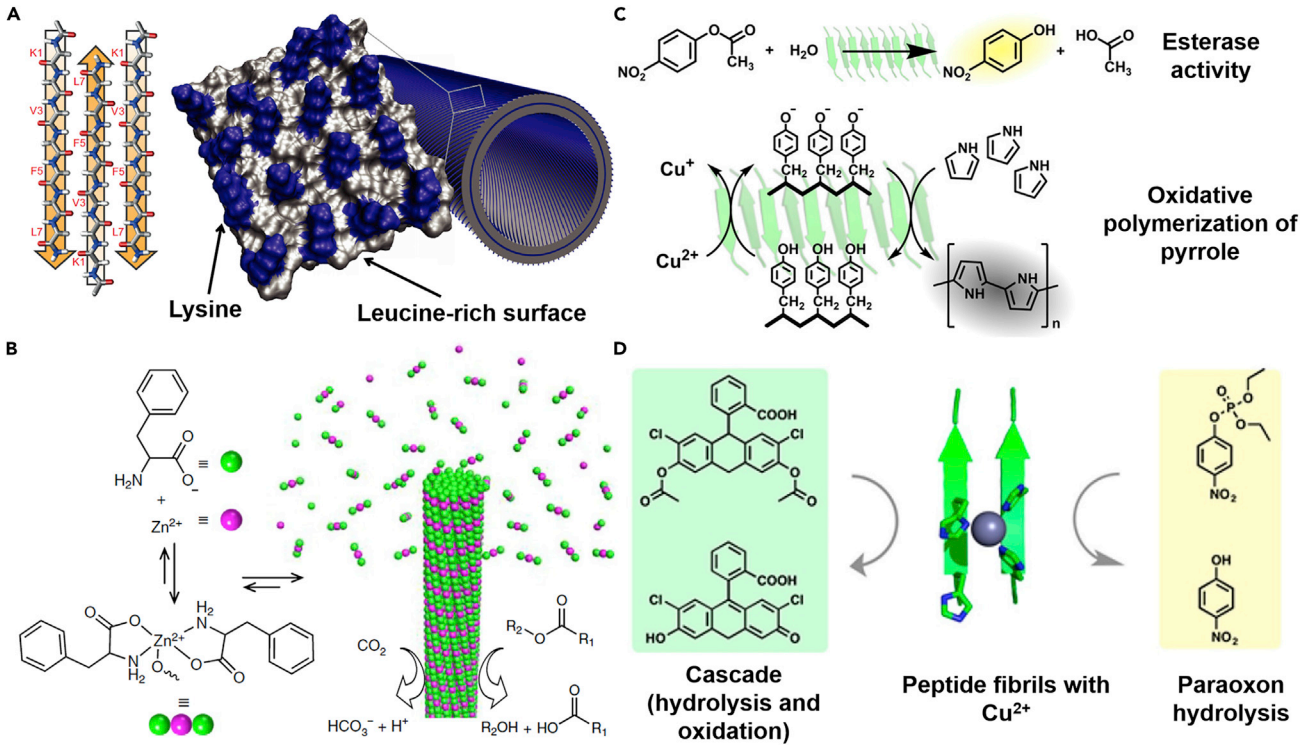

Figure 6. Multifunctional peptide-based supramolecular catalysts capable of orthogonal or cascade catalysis

(A) Self-assembly of K1 peptide into homogeneous amyloidal nanotube with exposed Lys (blue) and Leu (gray) residues. Reproduced with permission from ref.,[46] copyright 2017, Springer Nature.

(B) Co-assembly of Zn^{2+} ions and Phe for both CO_2 hydration and *p*-NPA hydrolysis. Reproduced with permission from ref.,[100] copyright 2019, Springer Nature.

(C) Self-assembled amyloid-like nanostructures for catalytic hydrolysis of *p*-NPA and electrocatalytic oxidative polymerization of pyrrole in the presence of Cu^{2+} ions. Reproduced with permission from ref.,[101] copyright 2021, American Chemical Society.

(D) Copper-containing peptide nanofibrils for paraoxon hydrolysis and cascade hydrolysis/oxidation reactions of DCFH-DA. Reproduced with permission from ref.,[102] copyright 2018, American Chemical Society.

homogeneous amyloidal nanotubes, on the surfaces of which high-density catalytic Lys residues and parallel cross-β grooves were uniformly arrayed (Figure 6A). Such self-assembled amyloid nanotubes exhibited the ability to catalyze different types of chemical reactions, including the water-mediated dimeric condensation of 6-amino-2-naphthaldehyde and enantioselective retro-aldol cleavage of methodol to 6-methoxy-2-naphthaldehyde. The enantioselectivity of the reactions arose from the chiroselective binding of *R*- and *S*-methodol by the cross-β grooves. For the retro-aldol reaction, the amyloid nanotubes showed an initial rate more than four orders of magnitude larger compared to the Lys alone.

Carbonic anhydrases (CAs) are a typical type of extant natural multifunctional metalloenzymes, which play a vital role in regulating internal pH and maintaining the acid-base homeostasis.[107] Natural CAs have the capacity for catalyzing both the reversible hydration of carbon dioxide (CO_2) and the hydrolysis of esters.[108,109] The active site of most CAs contains a Zn^{2+} ion that is coordinated with three His residues. Gazit and co-workers constructed a catalytic amyloid-like crystal structure through the co-assembly of Zn^{2+} ions and Phe under alkaline condition (Figure 6B), which could foster the CO_2 hydration as well as the *p*-NPA hydrolysis.[100] Notably, on the basis of molecular mass, the hydrolytic activity toward *p*-NPA of this self-assembled CAs mimic was even 8-fold greater than that of the natural CA II enzyme. Owing to the asymmetric arrangement of Zn^{2+} ions and Phe molecules in the crystal lattice, this CAs mimic displayed high stereoselectivity in the hydrolysis of $_L/_D$-Boc-phenylalanine 4-nitrophenyl ester ($_L/_D$-pNPA) enantiomers. Specifically, the hydrolysis rate of $_L$-pNPA was four times higher than that of $_D$-pNPA. Moreover, this CAs-mimicking artificial enzyme possessed remarkable substrate specificity, thermal stability, and reusability. This catalyst might supplement a link between the prebiotic amino acids and the primitive precursor enzymes.

Ventura and co-workers demonstrated that the short peptides consisting of repeated His-Tyr units at higher concentrations (seven to nine residues) can self-assemble to form amyloid-like nanofibrils or hydrogels.[101] These amyloid-like structures were capable of catalyzing both the hydrolysis reaction of *p*-NPA and the electrocatalytic oxidative polymerization of pyrrole in the presence of Cu^{2+} ions (Figure 6C). The hydrolytic activities were mainly dependent on the proximally located His residues, while the electrocatalytic activities basically arose from the adjacent Tyr residues and the Cu^{2+} ions. The architectures and the catalytic activities of this system were pH-responsive. It was catalytically active in self-assembled β-sheet nanofibrils at pH 8 but inactive in disassembled random coils at pH 4.

In consideration of the role of Cu^{2+} ions in both hydrolysis[110] and redox reactions, Korendovych and co-workers developed self-assembled amyloids consisting of the amyloid-forming heptapeptides (Ac-IHIHIYI-NH_2) and Cu^{2+} ions.[102] They observed the hydrolytic activity of the catalytic amyloids by employing paraoxon, a highly toxic organophosphate pesticide.[111] They used 2′,7′-dichlorofluorescin diacetate (DCFH-DA) to investigate the cascade catalytic properties of this amyloid (Figure 6D). There were two different pathways of transforming the DCFH-DA into fluorescent end-product 2′,7′-dichlorofluorescein (DCF), hydrolysis-oxidation or oxidation-hydrolysis. The overall rate of the second reaction pathway was slower. In another research, Das and co-workers fabricated a short peptide-based (Ac-HLVFFAL-$CONH_2$) amyloid nanotube with exposed His residues on its surface to bind hemin.[112] The adjacent His residues could serve as hydrolase mimic, and the His/hemin complex could act as peroxidase mimic. Using the 2-methoxy phenyl acetate (MPA) as substrate, cascade hydrolysis/oxidation reactions from MPA to end-product tetraguaiacol were observed.

Very recently, Jelinek and co-workers reported that the mature amyloid fibrils self-assembled from naturally occurring Aβ42 peptide efficiently catalyzed the hydrolysis of *p*-NPA and acetylthiocholine (a well-known surrogate for acetylcholine), as well as the oxidation of dopamine and adrenaline.[103] In comparison with the Aβ42 peptide, the monomers/oligomers or the fibrils comprised of Aβ42 subdomains displayed much lower catalytic activities toward the hydrolysis or oxidation. Noticeably, the acetylcholine, dopamine, and adrenaline are neurotransmitters, and the Aβ42 fibrils are the characteristic hallmarks of Alzheimer's disease (AD). The reaction products of these neurotransmitters, especially melanin (product of dopamine oxidation), have been identified in Parkinson's and AD patients. Therefore, this work implicated a possible relation between the natural peptide aggregation and *in vivo* pathological reactions.

The kinetic parameters of multifunctional enzyme mimics are listed in Table 1 (aldolase-like activities) and Table 4 (hydrolase-like activities).

Conclusions

In this review, we introduced the basic principle of constructing peptide-based supramolecular biomimetic catalysts through self-assembly of peptides. We discussed a variety of representative peptide-based artificial enzymes, which were fabricated aiming to mimic the active sites and catalytic properties of natural enzymes, such as aldolases, laccases, peroxidases, and hydrolases (mainly the esterases and phosphatases). Moreover, we described some multifunctional enzyme-mimetic system that were capable of catalyzing orthogonal or cascade reactions. The catalytic efficiency of several enzyme mimics rivaled, even outperformed, that of natural enzyme by weight. Some artificial enzymes displayed remarkable stability under harsh conditions or response to environmental stimuli. Furthermore, we highlighted the significance of these studies from an evolutionary point of view.

Despite some substantive progress, this field is at its preliminary stage. First, the catalytic efficiency of most peptide-based artificial enzymes is hardly on a par with their natural counterparts because the active sites in natural enzymes, especially the spatial position and orientation of reactive groups, are difficult to reproduce. Novel self-assembly strategies, with precise control over the distribution of reactive groups, are required. Second, the catalytic activities of peptide-based artificial enzymes are restricted to emulate only a few types of natural enzymes. We need to develop new peptide sequences and cofactors, as well as to exploit the co-assembly of multicomponent peptides, to expand the catalytic repertoire of supramolecular artificial enzymes. This may provide the possibility of constructing superior peptide-based multifunctional catalysts to realize cascade catalysis and even chemical reaction network. Third, there is still lack of well-defined structure-activity relationships that can instruct us to design the peptide-based artificial enzymes. On one hand, this requires advanced characterization techniques, for example, the

solid-state NMR (Nuclear Magnetic Resonance) and cryo-electron microscopy, which are able to provide detailed or even real-time structural information of the active sites. On the other hand, artificial intelligence (AI) and innovative theoretical simulation methods will also contribute to solve this problem.

ACKNOWLEDGMENTS

The authors are grateful for the financial support from National Natural Science Foundation of China (Grants 21872044 and 52173194), Fundamental Research Funds for the Central Universities (Grants XK1806, buctrc201902), and the FY2022 JSPS Postdoctoral Fellowship for Research in Japan (Standard) (Fellowship ID: P22051).

AUTHOR CONTRIBUTIONS

All authors wrote this review and made contributions to discussion of this review.

DECLARATION OF INTERESTS

The authors declare no competing interests.

INCLUSION AND DIVERSITY

We support inclusive, diverse, and equitable conduct of research.

REFERENCES

1. Goldsmith, M., and Tawfik, D.S. (2017). Enzyme engineering: reaching the maximal catalytic efficiency peak. Curr. Opin. Struct. Biol. *47*, 140–150. https://doi.org/10.1016/j.sbi.2017.09.002.

2. Hatzimanikatis, V., Li, C., Ionita, J.A., and Broadbelt, L.J. (2004). Metabolic networks: enzyme function and metabolite structure. Curr. Opin. Struct. Biol. *14*, 300–306. https://doi.org/10.1016/j.sbi.2004.04.004.

3. Noda-Garcia, L., Liebermeister, W., and Tawfik, D.S. (2018). Metabolite-enzyme coevolution: from single enzymes to metabolic pathways and networks. Annu. Rev. Biochem. *87*, 187–216. https://doi.org/10.1146/annurev-biochem-062917-012023.

4. Tawfik, D.S. (2014). Accuracy-rate tradeoffs: how do enzymes meet demands of selectivity and catalytic efficiency? Curr. Opin. Chem. Biol. *21*, 73–80. https://doi.org/10.1016/j.cbpa.2014.05.008.

5. Breaker, R.R. (2020). Imaginary ribozymes. ACS Chem. Biol. *15*, 2020–2030. https://doi.org/10.1021/acschembio.0c00214.

6. Cech, T.R. (2002). Ribozymes, the first 20 years. Biochem. Soc. Trans. *30*, 1162–1166. https://doi.org/10.1042/bst0301162.

7. Lilley, D.M.J. (2005). Structure, folding and mechanisms of ribozymes. Curr. Opin. Struct. Biol. *15*, 313–323. https://doi.org/10.1016/j.sbi.2005.05.002.

8. Baum, D.A., and Silverman, S.K. (2008). Deoxyribozymes: useful DNA catalysts in vitro and in vivo. Cell. Mol. Life Sci. *65*, 2156–2174. https://doi.org/10.1007/s00018-008-8029-y.

9. Silverman, S.K. (2009). Deoxyribozymes: selection design and serendipity in the development of DNA catalysts. Acc. Chem. Res. *42*, 1521–1531. https://doi.org/10.1021/ar900052y.

10. Silverman, S.K. (2016). Catalytic DNA: scope, applications, and biochemistry of deoxyribozymes. Trends Biochem. Sci. *41*, 595–609. https://doi.org/10.1016/j.tibs.2016.04.010.

11. Gladyshev, V.N., and Hatfield, D.L. (1999). Selenocysteine-containing proteins in mammals. J. Biomed. Sci. *6*, 151–160. https://doi.org/10.1007/BF02255899.

12. Turanov, A.A., Xu, X.M., Carlson, B.A., Yoo, M.H., Gladyshev, V.N., and Hatfield, D.L. (2011). Biosynthesis of selenocysteine, the 21st amino acid in the genetic code, and a novel pathway for cysteine biosynthesis. Adv. Nutr. *2*, 122–128. https://doi.org/10.3945/an.110.000265.

13. Gaston, M.A., Jiang, R., and Krzycki, J.A. (2011). Functional context, biosynthesis, and genetic encoding of pyrrolysine. Curr. Opin. Microbiol. *14*, 342–349. https://doi.org/10.1016/j.mib.2011.04.001.

14. Waldron, K.J., and Robinson, N.J. (2009). How do bacterial cells ensure that metalloproteins get the correct metal? Nat. Rev. Microbiol. *7*, 25–35. https://doi.org/10.1038/nrmicro2057.

15. Giles, N.M., Watts, A.B., Giles, G.I., Fry, F.H., Littlechild, J.A., and Jacob, C. (2003). Metal and redox modulation of cysteine protein function. Chem. Biol. *10*, 677–693. https://doi.org/10.1016/s1074-5521(03)00174-1.

16. Noda-Garcia, L., and Tawfik, D.S. (2020). Enzyme evolution in natural products biosynthesis: target- or diversity-oriented? Curr. Opin. Chem. Biol. *59*, 147–154. https://doi.org/10.1016/j.cbpa.2020.05.011.

17. Vaissier Welborn, V., and Head-Gordon, T. (2019). Computational design of synthetic enzymes. Chem. Rev. *119*, 6613–6630. https://doi.org/10.1021/acs.chemrev.8b00399.

18. Galanie, S., Entwistle, D., and Lalonde, J. (2020). Engineering biosynthetic enzymes for industrial natural product synthesis. Nat. Prod. Rep. *37*, 1122–1143. https://doi.org/10.1039/c9np00071b.

19. Luetz, S., Giver, L., and Lalonde, J. (2008). Engineered enzymes for chemical production. Biotechnol. Bioeng. *101*, 647–653. https://doi.org/10.1002/bit.22077.

20. Rehm, F.B.H., Chen, S., and Rehm, B.H.A. (2018). Bioengineering toward direct production of immobilized enzymes: a paradigm shift in biocatalyst design. Bioengineered *9*, 6–11. https://doi.org/10.1080/21655979.2017.1325040.

21. Jiao, Y., Shang, Y., Li, N., and Ding, B. (2022). DNA-based enzymatic systems and their applications. iScience *25*, 104018. https://doi.org/10.1016/j.isci.2022.104018.

22. Arnold, J., Chapman, J., Arnold, M., and Dinu, C.Z. (2022). Hyaluronic acid allows enzyme immobilization for applications in biomedicine. Biosensors *12*, 28. https://doi.org/10.3390/bios12010028.

23. Shekhter, A.B., Balakireva, A.V., Kuznetsova, N.V., Vukolova, M.N., Litvitsky, P.F., and Zamyatnin, A.A. (2019). Collagenolytic enzymes and their applications in biomedicine. Curr. Med. Chem. *26*, 487–505. https://doi.org/10.2174/0929867324666171006124236.

24. Vellard, M. (2003). The enzyme as drug: application of enzymes as pharmaceuticals. Curr. Opin. Biotechnol. *14*, 444–450. https://doi.org/10.1016/s0958-1669(03)00092-2.

25. Kaushal, J., Mehandia, S., Singh, G., Raina, A., and Arya, S.K. (2018). Catalase enzyme: application in bioremediation and food industry. Biocatal. Agric. Biotechnol. *16*, 192–199. https://doi.org/10.1016/j.bcab.2018.07.035.

26. Nahar, S., Mizan, M.F.R., Ha, A.J.W., and Ha, S.D. (2018). Advances and future prospects of enzyme-based biofilm prevention approaches in the food industry. Compr. Rev. Food Sci. Food Saf. *17*, 1484–1502. https://doi.org/10.1111/1541-4337.12382.

27. Du, P., Xu, S., Xu, Z., and Wang, Z. (2021). Bioinspired self-assembling materials for modulating enzyme functions. Adv. Funct. Mater. *31*, 2104819. https://doi.org/10.1002/adfm.202104819.

28. Hamley, I.W. (2021). Biocatalysts based on peptide and peptide conjugate nanostructures. Biomacromolecules *22*, 1835–1855. https://doi.org/10.1021/acs.biomac.1c00240.

29. Han, J., Gong, H., Ren, X., and Yan, X. (2021). Supramolecular nanozymes based on peptide self-assembly for biomimetic catalysis. Nano Today *41*, 101295. https://doi.org/10.1016/j.nantod.2021.101295.

30. Liu, S., Du, P., Sun, H., Yu, H.Y., and Wang, Z.G. (2020). Bioinspired supramolecular catalysts from designed self-assembly of DNA or peptides. ACS Catal. *10*, 14937–14958. https://doi.org/10.1021/acscatal.0c03753.

31. Marshall, L.R., and Korendovych, I.V. (2021). Catalytic amyloids: is misfolding folding? Curr. Opin. Chem. Biol. *64*, 145–153. https://doi.org/10.1016/j.cbpa.2021.06.010.

32. Zozulia, O., Dolan, M.A., and Korendovych, I.V. (2018). Catalytic peptide assemblies. Chem. Soc. Rev. *47*, 3621–3639. https://doi.org/10.1039/c8cs00080h.

33. Chatterjee, A., Reja, A., Pal, S., and Das, D. (2022). Systems chemistry of peptide-assemblies for biochemical transformations. Chem. Soc. Rev. *51*, 3047–3070. https://doi.org/10.1039/d1cs01178b.

34. Copley, S.D. (2012). Toward a systems biology perspective on enzyme evolution. J. Biol. Chem. *287*, 3–10. https://doi.org/10.1074/jbc.R111.254714.

35. Radman, M. (1999). Enzymes of evolutionary change. Nature *401*, 866–867. https://doi.org/10.1038/44738.

36. Fessner, W.D., and Helaine, V. (2001). Biocatalytic synthesis of hydroxylated natural products using aldolases and related enzymes. Curr. Opin. Biotechnol. *12*, 574–586. https://doi.org/10.1016/s0958-1669(01)00265-8.

37. Windle, C.L., Müller, M., Nelson, A., and Berry, A. (2014). Engineering aldolases as biocatalysts. Curr. Opin. Chem. Biol. *19*, 25–33. https://doi.org/10.1016/j.cbpa.2013.12.010.

38. Fessner, W.D., Schneider, A., Held, H., Sinerius, G., Walter, C., Hixon, M., and Schloss, J.V. (1996). The mechanism of class II, metal-dependent aldolases. Angew. Chem., Int. Ed. Engl. *35*, 2219–2221. https://doi.org/10.1002/anie.199622191.

39. Gefflaut, T., Blonski, C., Perie, J., and Willson, M. (1995). Class I aldolases: substrate specificity, mechanism, inhibitors and structural aspects. Prog. Biophys. Mol. Biol. *63*, 301–340. https://doi.org/10.1016/0079-6107(95)00008-9.

40. Müller, M.M., Windsor, M.A., Pomerantz, W.C., Gellman, S.H., and Hilvert, D. (2009). A rationally designed aldolase foldamer. Angew. Chem. Int. Ed. Engl. *48*, 922–925. https://doi.org/10.1002/anie.200804996.

41. Rodríguez-Llansola, F., Escuder, B., and Miravet, J.F. (2009). Switchable perfomance of an L-proline-derived basic catalyst controlled by supramolecular gelation. J. Am. Chem. Soc. *131*, 11478–11484. https://doi.org/10.1021/ja902589f.

42. Reja, A., Afrose, S.P., and Das, D. (2020). Aldolase cascade facilitated by self-assembled nanotubes from short peptide amphiphiles. Angew. Chem. Int. Ed. Engl. *59*, 4329–4334. https://doi.org/10.1002/anie.201914633.

43. Jiang, L., Althoff, E.A., Clemente, F.R., Doyle, L., Röthlisberger, D., Zanghellini, A., Gallaher, J.L., Betker, J.L., Tanaka, F., Barbas, C.F., et al. (2008). De novo computational design of retro-aldol enzymes. Science *319*, 1387–1391. https://doi.org/10.1126/science.1152692.

44. Duschmalé, J., Kohrt, S., and Wennemers, H. (2014). Peptide catalysis in aqueous emulsions. Chem. Commun. *50*, 8109–8112. https://doi.org/10.1039/c4cc01759e.

45. Tena-Solsona, M., Nanda, J., Díaz-Oltra, S., Chotera, A., Ashkenasy, G., and Escuder, B. (2016). Emergent catalytic behavior of self-assembled low molecular weight peptide-based aggregates and hydrogels. Chemistry *22*, 6687–6694. https://doi.org/10.1002/chem.201600344.

46. Omosun, T.O., Hsieh, M.C., Childers, W.S., Das, D., Mehta, A.K., Anthony, N.R., Pan, T., Grover, M.A., Berland, K.M., and Lynn, D.G. (2017). Catalytic diversity in self-propagating peptide assemblies. Nat. Chem. *9*, 805–809. https://doi.org/10.1038/nchem.2738.

47. Hawkins, K., Patterson, A.K., Clarke, P.A., and Smith, D.K. (2020). Catalytic gels for a prebiotically relevant asymmetric aldol reaction in water: from organocatalyst design to hydrogel discovery and back again. J. Am. Chem. Soc. *142*, 4379–4389. https://doi.org/10.1021/jacs.9b13156.

48. Pelin, J.N.B.D., Gerbelli, B.B., Edwards-Gayle, C.J.C., Aguilar, A.M., Castelletto, V., Hamley, I.W., and Alves, W.A. (2020). Amyloid peptide mixtures: self-assembly, hydrogelation, nematic ordering, and catalysts in aldol reactions. Langmuir *36*, 2767–2774. https://doi.org/10.1021/acs.langmuir.0c00198.

49. Claus, H. (2004). Laccases: structure, reactions, distribution. Micron *35*, 93–96. https://doi.org/10.1016/j.micron.2003.10.029.

50. Mayer, A.M., and Staples, R.C. (2002). Laccase: new functions for an old enzyme. Phytochemistry *60*, 551–565. https://doi.org/10.1016/s0031-9422(02)00171-1.

51. Jones, S.M., and Solomon, E.I. (2015). Electron transfer and reaction mechanism of laccases. Cell. Mol. Life Sci. *72*, 869–883. https://doi.org/10.1007/s00018-014-1826-6.

52. Li, H., Webb, S.P., Ivanic, J., and Jensen, J.H. (2004). Determinants of the relative reduction potentials of type-1 copper sites in proteins. J. Am. Chem. Soc. *126*, 8010–8019. https://doi.org/10.1021/ja049345y.

53. Zovo, K., Pupart, H., Van Wieren, A., Gillilan, R.E., Huang, Q., Majumdar, S., and Lukk, T. (2022). Substitution of the methionine axial ligand of the T1 copper for the fungal-like phenylalanine ligand (M298F) causes local structural perturbations that lead to thermal instability and reduced catalytic efficiency of the small laccase from streptomyces coelicolor A3(2). ACS Omega *7*, 6184–6194. https://doi.org/10.1021/acsomega.1c06668.

54. Makhlynets, O.V., Gosavi, P.M., and Korendovych, I.V. (2016). Short self-assembling peptides are able to bind to copper and activate oxygen. Angew. Chem. Int. Ed. Engl. *55*, 9017–9020. https://doi.org/10.1002/anie.201602480.

55. Wang, J., Huang, R., Qi, W., Su, R., Binks, B.P., and He, Z. (2019). Construction of a bioinspired laccase-mimicking nanozyme for the degradation and detection of phenolic pollutants. Appl. Catal. B Environ. *254*, 452–462. https://doi.org/10.1016/j.apcatb.2019.05.012.

56. Makam, P., Yamijala, S.S.R.K.C., Bhadram, V.S., Shimon, L.J.W., Wong, B.M., and Gazit, E. (2022). Single amino acid bionanozyme for environmental remediation. Nat. Commun. *13*, 1505. https://doi.org/10.1038/s41467-022-28942-0.

57. Maury, C.P.J. (2009). Self-propagating beta-sheet polypeptide structures as prebiotic informational molecular entities: the amyloid world. Orig. Life Evol. Biosph. *39*, 141–150. https://doi.org/10.1007/s11084-009-9165-6.

58. Maury, C.P.J. (2018). Amyloid and the origin of life: self-replicating catalytic amyloids as prebiotic informational and protometabolic entities. Cell. Mol. Life Sci. *75*, 1499–1507. https://doi.org/10.1007/s00018-018-2797-9.

59. Xu, X., Wang, J., Huang, R., Qi, W., Su, R., and He, Z. (2021). Preparation of laccase mimicking nanozymes and their catalytic oxidation of phenolic pollutants. Catal. Sci. Technol. *11*, 3402–3410. https://doi.org/10.1039/d1cy00074h.

60. Banci, L. (1997). Structural properties of peroxidases. J. Biotechnol. *53*, 253–263. https://doi.org/10.1016/s0168-1656(97)01677-5.

61. Fülöp, V., Ridout, C.J., Greenwood, C., and Hajdu, J. (1995). Crystal structure of the di-haem cytochrome c peroxidase from Pseudomonas aeruginosa. Structure *3*, 1225–1233. https://doi.org/10.1016/s0969-2126(01)00258-1.

62. Veitch, N.C. (2004). Horseradish peroxidase: a modern view of a classic enzyme. Phytochemistry *65*, 249–259. https://doi.org/10.1016/j.phytochem.2003.10.022.

63. Wang, Q., Yang, Z., Zhang, X., Xiao, X., Chang, C.K., and Xu, B. (2007). A supramolecular-hydrogel-encapsulated hemin as an artificial enzyme to mimic peroxidase. Angew. Chem. Int. Ed. Engl. *46*, 4285–4289. https://doi.org/10.1002/anie.200700404.

64. Wang, Q., Yang, Z., Ma, M., Chang, C.K., and Xu, B. (2008). High catalytic activities of artificial peroxidases based on supramolecular hydrogels that contain heme models. Chemistry *14*, 5073–5078. https://doi.org/10.1002/chem.200702010.

65. Mahajan, M., and Bhattacharjya, S. (2013). Beta-hairpin peptides: heme binding, catalysis, and structure in detergent micelles. Angew. Chem. Int. Ed. Engl. *52*, 6430–6434. https://doi.org/10.1002/anie.201300241.

66. D'Souza, A., Wu, X., Yeow, E.K.L., and Bhattacharjya, S. (2017). Designed heme-cage beta-sheet miniproteins. Angew. Chem., Int. Ed. Engl. *56*, 5904–5908. https://doi.org/10.1002/anie.201702472.

67. Geng, R., Chang, R., Zou, Q., Shen, G., Jiao, T., and Yan, X. (2021). Biomimetic nanozymes based on coassembly of amino acid and hemin for catalytic oxidation and sensing of biomolecules. Small *17*, 2008114. https://doi.org/10.1002/smll.202008114.

68. Jian, T., Zhou, Y., Wang, P., Yang, W., Mu, P., Zhang, X., Zhang, X., and Chen, C.L. (2022). Highly stable and tunable peptoid/hemin enzymatic mimetics with natural peroxidase-like activities. Nat. Commun. *13*, 3025. https://doi.org/10.1038/s41467-022-30285-9.

69. Liu, Q., Wan, K., Shang, Y., Wang, Z.G., Zhang, Y., Dai, L., Wang, C., Wang, H., Shi, X., Liu, D., and Ding, B. (2021). Cofactor-free oxidase-mimetic nanomaterials from self-assembled histidine-rich peptides. Nat. Mater. *20*, 395–402. https://doi.org/10.1038/s41563-020-00856-6.

70. Feng, Y., Wang, Y., Zhang, J., Wang, M., Qi, W., Su, R., and He, Z. (2019). Self-assembly of ferrocene peptides: a nonheme strategy to construct a peroxidase mimic. Adv. Mater. Interfac. *6*, 1901082. https://doi.org/10.1002/admi.201901082.

71. Zozulia, O., Marshall, L.R., Kim, I., Kohn, E.M., and Korendovych, I.V. (2021). Self-assembling catalytic peptide nanomaterials capable of highly efficient peroxidase activity. Chemistry *27*, 5388–5392. https://doi.org/10.1002/chem.202100182.

72. Liu, Y., Du, P., Teng, Q., Sun, H., Ye, X., and Wang, Z.-G. (2022). Self-assembly of fibril-forming histidine-rich peptides for cofactor-free oxidase-mimetic catalysis. Supramolecular Materials *1*, 100012. https://doi.org/10.1016/j.supmat.2022.100012.

73. Du, P., Liu, S., Sun, H., Wu, H., and Wang, Z.G. (2022). Designed histidine-rich peptide self-assembly for accelerating oxidase-catalyzed reactions. Nano Res. *15*, 4032–4038. https://doi.org/10.1007/s12274-022-4209-6.

74. Liu, Q., Wang, H., Shi, X., Wang, Z.G., and Ding, B. (2017). Self-assembled DNA/peptide-based nanoparticle exhibiting synergistic enzymatic activity. ACS Nano *11*, 7251–7258. https://doi.org/10.1021/acsnano.7b03195.

75. Sun, H., Wu, H., Teng, Q., Liu, Y., Wang, H., and Wang, Z.G. (2022). Enzyme-mimicking materials from designed self-assembly of lysine-rich peptides and G-quadruplex DNA/hemin DNAzyme: charge effect of the key residues on the catalytic functions. Biomacromolecules *23*, 3469–3476. https://doi.org/10.1021/acs.biomac.2c00620.

76. Teng, Q., Wu, H., Sun, H., Liu, Y., Wang, H., and Wang, Z.G. (2022). Switchable enzyme-mimicking catalysts self-assembled from de novo designed peptides and DNA G-quadruplex/hemin complex. J. Colloid Interface Sci. *628*, 1004–1011. https://doi.org/10.1016/j.jcis.2022.08.005.

77. Wang, Z.G., Wang, H., Liu, Q., Duan, F., Shi, X., and Ding, B. (2018). Designed self-assembly of peptides with G-quadruplex/hemin DNAzyme into nanofibrils possessing enzyme-mimicking active sites and catalytic functions. ACS Catal. *8*, 7016–7024. https://doi.org/10.1021/acscatal.8b00896.

78. Paasche, A., Zipper, A., Schäfer, S., Ziebuhr, J., Schirmeister, T., and Engels, B. (2014). Evidence for substrate binding-induced zwitterion formation in the catalytic Cys-His dyad of the SARS-CoV main protease. Biochemistry *53*, 5930–5946. https://doi.org/10.1021/bi400604t.

79. Litzinger, S., Fischer, S., Polzer, P., Diederichs, K., Welte, W., and Mayer, C. (2010). Structural and kinetic analysis of Bacillus subtilis N-acetylglucosaminidase reveals a unique Asp-His dyad mechanism. J. Biol. Chem. *285*, 35675–35684. https://doi.org/10.1074/jbc.M110.131037.

80. Ekici, O.D., Paetzel, M., and Dalbey, R.E. (2008). Unconventional serine proteases: variations on the catalytic Ser/His/Asp triad configuration. Protein Sci. *17*, 2023–2037. https://doi.org/10.1110/ps.035436.108.

81. Buller, A.R., and Townsend, C.A. (2013). Intrinsic evolutionary constraints on protease structure, enzyme acylation, and the identity of the catalytic triad. Proc. Natl. Acad. Sci. USA *110*, E653–E661. https://doi.org/10.1073/pnas.1221050110.

82. Manjasetty, B.A., Büssow, K., Fieber-Erdmann, M., Roske, Y., Gobom, J., Scheich, C., Götz, F., Niesen, F.H., and Heinemann, U. (2006). Crystal structure of Homo sapiens PTD012 reveals a zinc-containing hydrolase fold. Protein Sci. *15*, 914–920. https://doi.org/10.1110/ps.052037006.

83. Vallee, B.L., and Auld, D.S. (1993). Zinc - biological functions and coordination motifs. Acc. Chem. Res. *26*, 543–551. https://doi.org/10.1021/ar00034a005.

84. Guler, M.O., and Stupp, S.I. (2007). A self-assembled nanofiber catalyst for ester hydrolysis. J. Am. Chem. Soc. *129*, 12082–12083. https://doi.org/10.1021/ja075044n.

85. Rufo, C.M., Moroz, Y.S., Moroz, O.V., Stöhr, J., Smith, T.A., Hu, X., DeGrado, W.F., and Korendovych, I.V. (2014). Short peptides self-assemble to produce catalytic amyloids. Nat. Chem. *6*, 303–309. https://doi.org/10.1038/nchem.1894.

86. Zhang, C., Xue, X., Luo, Q., Li, Y., Yang, K., Zhuang, X., Jiang, Y., Zhang, J., Liu, J., Zou, G., and Liang, X.J. (2014). Self-assembled peptide nanofibers designed as biological enzymes for catalyzing ester hydrolysis. ACS Nano *8*, 11715–11723. https://doi.org/10.1021/nn5051344.

87. Zhang, C., Shafi, R., Lampel, A., MacPherson, D., Pappas, C.G., Narang, V., Wang, T., Maldarelli, C., and Ulijn, R.V. (2017). Switchable hydrolase based on reversible formation of supramolecular catalytic site using a self-assembling peptide. Angew. Chem., Int. Ed. Engl. *56*, 14511–14515. https://doi.org/10.1002/anie.201708036.

88. Wang, Y., Yang, L., Wang, M., Zhang, J., Qi, W., Su, R., and He, Z. (2021). Bioinspired phosphatase-like mimic built from the self-assembly of de novo designed helical short peptides. ACS Catal. *11*, 5839–5849. https://doi.org/10.1021/acscatal.1c00129.

89. Al-Garawi, Z.S., McIntosh, B.A., Neill-Hall, D., Hatimy, A.A., Sweet, S.M., Bagley, M.C., and Serpell, L.C. (2017). The amyloid architecture provides a scaffold for enzyme-like catalysts. Nanoscale *9*, 10773–10783. https://doi.org/10.1039/c7nr02675g.

90. Zhao, Y., Lei, B., Wang, M., Wu, S., Qi, W., Su, R., and He, Z. (2018). A supramolecular approach to construct a hydrolase mimic with photo-switchable catalytic activity. J. Mater. Chem. B *6*, 2444–2449. https://doi.org/10.1039/c8tb00448j.

91. Wang, M., Lv, Y., Liu, X., Qi, W., Su, R., and He, Z. (2016). Enhancing the activity of peptide-based artificial hydrolase with catalytic Ser/His/Asp triad and molecular imprinting. ACS Appl. Mater. Interfaces *8*, 14133–14141. https://doi.org/10.1021/acsami.6b04670.

92. Gulseren, G., Khalily, M.A., Tekinay, A.B., and Guler, M.O. (2016). Catalytic supramolecular self-assembled peptide nanostructures for ester hydrolysis. J. Mater. Chem. B *4*, 4605–4611. https://doi.org/10.1039/c6tb00795c.

93. Sarkhel, B., Chatterjee, A., and Das, D. (2020). Covalent catalysis by cross beta amyloid nanotubes. J. Am. Chem. Soc. *142*, 4098–4103. https://doi.org/10.1021/jacs.9b13517.

94. Razkin, J., Nilsson, H., and Baltzer, L. (2007). Catalysis of the cleavage of uridine 3′-2, 2, 2-trichloroethylphosphate by a designed helix-loop-helix motif peptide. J. Am. Chem. Soc. *129*, 14752–14758. https://doi.org/10.1021/ja075478i.

95. Razkin, J., Lindgren, J., Nilsson, H., and Baltzer, L. (2008). Enhanced complexity and catalytic efficiency in the hydrolysis of phosphate diesters by rationally designed helix-loop-helix motifs. Chembiochem *9*, 1975–1984. https://doi.org/10.1002/cbic.200800057.

96. O'Brien, P.J., and Herschlag, D. (2002). Alkaline phosphatase revisited: hydrolysis of alkyl phosphates. Biochemistry *41*, 3207–3225. https://doi.org/10.1021/bi012166y.

97. Gulseren, G., Yasa, I.C., Ustahuseyin, O., Tekin, E.D., Tekinay, A.B., and Guler, M.O. (2015). Alkaline phosphatase-mimicking peptide nanofibers for osteogenic differentiation. Biomacromolecules *16*, 2198–2208. https://doi.org/10.1021/acs.biomac.5b00593.

98. Singh, A., Joseph, J.P., Gupta, D., Miglani, C., Mavlankar, N.A., and Pal, A. (2021). Photothermally switchable peptide nanostructures towards modulating catalytic hydrolase activity. Nanoscale *13*, 13401–13409. https://doi.org/10.1039/D1NR03655F.

99. Gupta, D., Sasmal, R., Singh, A., Joseph, J.P., Miglani, C., Agasti, S.S., and Pal, A. (2020). Enzyme-responsive chiral self-sorting in amyloid-inspired minimalistic peptide amphiphiles. Nanoscale *12*, 18692–18700. https://doi.org/10.1039/D0NR04581K.

100. Makam, P., Yamijala, S.S.R.K.C., Tao, K., Shimon, L.J.W., Eisenberg, D.S., Sawaya, M.R., Wong, B.M., and Gazit, E. (2019). Non-proteinaceous hydrolase comprised of a phenylalanine metallo-supramolecular amyloid-like structure. Nat. Catal. *2*, 977–985. https://doi.org/10.1038/s41929-019-0348-x.

101. Díaz-Caballero, M., Navarro, S., Nuez-Martínez, M., Peccati, F., Rodríguez-Santiago, L., Sodupe, M., Teixidor, F., and Ventura, S. (2021). pH-Responsive self-assembly of amyloid fibrils for dual hydrolase-oxidase reactions. ACS Catal. *11*, 595–607. https://doi.org/10.1021/acscatal.0c03093.

102. Lengyel, Z., Rufo, C.M., Moroz, Y.S., Makhlynets, O.V., and Korendovych, I.V. (2018). Copper-containing catalytic amyloids promote phosphoester hydrolysis and tandem reactions. ACS Catal. *8*, 59–62. https://doi.org/10.1021/acscatal.7b03323.

103. Arad, E., Baruch Leshem, A., Rapaport, H., and Jelinek, R. (2021). β-Amyloid fibrils catalyze neurotransmitter degradation. Chem Catalysis *1*, 908–922. https://doi.org/10.1016/j.checat.2021.07.005.

104. Carbonell, P., Lecointre, G., and Faulon, J.L. (2011). Origins of specificity and promiscuity in metabolic networks. J. Biol. Chem. *286*, 43994–44004. https://doi.org/10.1074/jbc.M111.274050.

105. Hult, K., and Berglund, P. (2007). Enzyme promiscuity: mechanism and applications. Trends Biotechnol. *25*, 231–238. https://doi.org/10.1016/j.tibtech.2007.03.002.

106. Khersonsky, O., Roodveldt, C., and Tawfik, D.S. (2006). Enzyme promiscuity: evolutionary and mechanistic aspects. Curr. Opin. Chem. Biol. *10*, 498–508. https://doi.org/10.1016/j.cbpa.2006.08.011.

107. Mboge, M.Y., Mahon, B.P., McKenna, R., and Frost, S.C. (2018). Carbonic anhydrases: role in pH control and cancer. Metabolites *8*, 19. https://doi.org/10.3390/metabo8010019.

108. Angeli, A., Carta, F., and Supuran, C.T. (2020). Carbonic anhydrases: versatile and useful biocatalysts in chemistry and biochemistry. Catalysts *10*, 1008. https://doi.org/10.3390/catal10091008.

109. Supuran, C.T. (2016). Structure and function of carbonic anhydrases. Biochem. J. *473*, 2023–2032. https://doi.org/10.1042/BCJ20160115.

110. Mortland, M.M., and Raman, K.V. (1967). Catalytic hydrolysis of some organic phosphate pesticides by copper (II). J. Agric. Food Chem. *15*, 163–167. https://doi.org/10.1021/jf60149a015.

111. Sobolev, V.E., Sokolova, M.O., Jenkins, R.O., and Goncharov, N.V. (2021). Nephrotoxic effects of paraoxon in three rat models of acute intoxication. Int. J. Mol. Sci. *22*, 13625. https://doi.org/10.3390/ijms222413625.

112. Chatterjee, A., Afrose, S.P., Ahmed, S., Venugopal, A., and Das, D. (2020). Cross-beta amyloid nanotubes for hydrolase-peroxidase cascade reactions. Chem. Commun. *56*, 7869–7872. https://doi.org/10.1039/d0cc00279h.